Conformational Activation of Acylpapains and Acylcathepsin B's: Resonance Raman and Kinetic Evidence†

R. H. Angus, P. R. Carey,* H. Lee, and A. C. Storer
Division of Biological Sciences, National Research Council of Canada, Ottawa, Ontario, Canada K1A 0R6
Received October 28, 1985; Revised Manuscript Received January 23, 1986

ABSTRACT: It is shown that, by extending the size of the substrate to meet papain's specificity requirement, conformational changes occur in bonds adjacent to the scissile linkage in the acyl enzyme. The resonance Raman (RR) spectra of the dithioacylpapains $CH_3OC(=O)$-Phe-$NHCH_2C(=S)$S-papain, $CH_3OC(=O)$-Gly-Phe-$NHCH_2C(=S)$S-papain, and $CH_3OC(=O)$-Gly-Gly-Phe-$NHCH_2C(=S)$S-papain, formed from thiono ester substrates, are found to be very similar, indicating that each dithioacyl enzyme takes up an identical B-type conformation in the $-NHCH_2C(=S)SCH_2-$ linkages. Moreover, the k_{cat} and k_{cat}/K_m parameters for the reactions involving these intermediates are similar (in the ranges 0.51–0.67 s^{-1} and 44 100–68 200 M^{-1} s^{-1}, respectively). For these reactions $k_{cat} = k_3$, the rate constant for deacylation. The strong structural similarities in the region undergoing catalytic transformation, taken with the similar k_3's, show that placing glycine residues in papain's S_3 and S_4 subsites has little effect on the deacylation process. However, there are marked RR spectral and kinetic differences between the intermediates formed from these three substrates, all of which meet papain's requirement for Phe at the S_2 subsite, and *N*-(β-phenylpropionyl)glycine dithioacylpapain, $C_6H_5(CH_2)_2C(=O)NHCH_2C(=S)$S-papain. The RR spectral differences indicate that changes occur in the torsional angles of the $-NH-CH_2-C(=S)-S-CH_2-$ fragment upon going to the di-, tri-, and tetrapeptide-based substrates. The changes in these torsional angles are consistent with slight conformational activation since higher k_3 values are found for the di-, tri-, and tetrapeptide-based substrates (0.51–0.67 s^{-1}) compared to the k_3 for $C_6H_5(CH_2)_2C(=O)NHCH_2C(=S)$S-papain of 0.165 s^{-1}. The kinetic and spectroscopic data show that enzyme–substrate contacts at the $-C(=O)NH$-Phe-Gly peptide linkage are important in fine tuning the structure near the scissile bond for favorable deacylation. The analysis of the RR spectra of the dithioacylpapains is supported by RR data from the corresponding ethyl dithio esters in solution and in the solid phase. RR and kinetic data are also compared for the dithioacyl enzymes formed from porcine spleen cathepsin B and the tri- and tetrapeptide thiono ester substrates. The RR spectra show that the substrates take up B-type conformations in the $-NHCH_2C(=S)SCH_2-$ fragment identical with that found for the papain analogues. This fact taken with the similarities in k_3 values supports the concept that the deacylation process is strongly conserved in going from plant to mammalian cysteine proteinases.

Enzyme–substrate contacts distant from the point where catalytic transformation occurs can have a marked effect on kinetic parameters. For example, Thompson (1974) has shown that contacts in the S_4–S_5 region of elastase can bring about an increase in the rate of hydrolysis, k_{cat}, of the amide link of the substrate bound at the S_1–P_1 position of 94-fold. In a review of proton inventory studies, Venkatasubban and Schowen (1984) concluded that for the serine proteases proper activation of the charge-relay apparatus requires an extensive set of enzyme–substrate interactions, involving not only those at the scissile residue but also those at remote subsites. However, the changes at the molecular level that accompany such kinetic effects are poorly understood. For this reason we have undertaken a comparison of a series of substrates that successively fill the S_1 to S_4 subsites of the cysteine proteinase papain. The steady-state kinetic parameters for these reactions have been obtained. At the same time, by using substrates that are thiono esters ($RC(=S)OCH_3$), we have been able to generate enzyme–substrate intermediates that are dithioacyl enzymes, RC(=S)S-papain. The chromophoric nature of the dithio ester linkage provides a "handle" by which to obtain the resonance Raman (RR) spectra of the dithioacyl enzymes (Carey & Storer 1984, 1985). Since the RR spectra provide detailed structural information on the critical $CH_2-C(=S)-S-CH_2$ bonds, we can attempt to relate changes in kinetic parameters for the series of substrates to changes in structure at the point of catalytic transformation. It is known that papain prefers a hydrophobic residue, particularly the phenylalanine side chain ($C_6H_5CH_2-$), at the S_2 position (Schecter & Berger, 1968). Thus, we have chosen to compare the series of substrates $C_6H_5(CH_2)_2C(=O)NHCH_2C(=S)OCH_3$, $CH_3OC(=O)$-Phe-$NHCH_2C(=S)OCH_3$, $CH_3OC(=O)$-Gly-Phe-$NHCH_2C(=S)OCH_3$, and $CH_3OC(=O)$-Gly-Gly-Phe-$NHCH_2C(=S)OCH_3$. The series goes successively from a single amino acid based substrate [blocked by a phenylalanine analogue, $C_6H_5(CH_2)_2-$] to a tetrapeptide-based thiono ester.

Additionally, in a continuation of earlier work (Carey et al., 1984) the tri- and tetrapeptide-based substrates have been used to compare the RR spectroscopic, structural, and kinetic properties of the dithioacyl enzymes formed by papain and the lysosomal mammalian proteinase cathepsin B. This comparison provides a critical test of the functional homology for a plant cysteine proteinase and a mammalian cysteine proteinase at the acyl enzyme stage of the reaction.

Experimental Procedures

Materials. Papain and pig spleen cathepsin B were prepared, activated, and assayed as described previously (Carey et al., 1984).

† NRCC No. 25 589.

0006-2960/86/0425-3304$01.50/0

Substrate and Dithio Ester Preparation. The *N*-(methyloxy)carbonyl derivatives of phenylalanine, glycylphenylalanine, and glycylglycylphenylalanine were prepared by treatment with methyl chloroformate (Carey et al., 1984). *N*-[(Methyloxy)carbonyl]phenylalanylglycine methyl ester, *N*-[(methyloxy)carbonyl]glycylphenylalanylglycine methyl ester, and *N*-[(methyloxy)carbonyl]glycylglycylphenylalanylglycine methyl ester and the corresponding nitriles were prepared by the mixed anhydride method (Lowe & Yuthavong, 1971; Anderson et al., 1967). The thiono esters and dithio esters were prepared from the nitriles as previously described (Carey et al., 1984).

All methyl, methyl thiono, and ethyl dithio esters of these peptides were checked for purity by NMR, and the results of their elemental analysis agreed, within acceptable limits (±0.02 times the calculated percentage), with the theoretical values.

Methods. Resonance Raman spectra were measured on a Spex Triplemate equipped with a Tracor Northern DARSS (diode array rapid scan spectrometer system). The spectrograph stage of the Triplemate employs a 3600 g/mm holographic grating, resulting in an approximately 900-cm^{-1} spectral range displayed across the diode array in the 335-nm region. The 324-nm line of a Coherent Radiation 2000K krypton ion laser was used as an excitation source. The apparatus is described in detail elsewhere (Carey & Sans Cartier, 1983). Raman frequencies were calibrated by using two emission lines from an argon lamp that correspond to Raman shifts of 742.5 and 1225.9 cm^{-1} with 324-nm excitation. Absolute accuracy of the calibrated wavenumbers is believed to be within ±2 cm^{-1}. For sequential spectra reproducibility is better than ±1 cm^{-1}.

For solution spectra the sample cell consisted of a quartz cuvette (0.5-cm path length), stirred by a magnetic pip during measurement to avoid photodegradation. In a typical reaction mixture 60 μL of 25 mM substrate (in 50% CH_3CN/H_2O; final concentration of CH_3CN, 10%) was added to 240 μL of enzyme [130 μM, pH 6.0, 1 mM ethylenediaminetetraacetic acid (EDTA)]. Data collection commenced a few seconds after mixing. RR spectra of the dithio esters in the solid state were obtained by coating the inside of a quartz NMR tube with powdered sample, spinning the tube in the vertical position by using an NMR spinner, and collecting the Raman photons in the backscattering geometry.

pH-Stat Kinetics. All pH-state measurements were performed at 20 °C. For methyl esters and methyl thiono esters, initial rates were measured on a Radiometer RTS822 recording titration system. The reaction mixture contained 0.3 M NaCl, 1 mM EDTA, and 20% acetonitrile in 20 mL for papain and 10% acetonitrile in 5 mL for cathepsin B. The rate was determined by monitoring the addition of a standardized NaOH solution. Initial rates were measured at a range of substrate concentrations of 0.01–0.15 mM for the methyl thiono esters and 0.2–2.0 mM for the methyl esters. Plots of s/v vs. s were linear, and kinetic parameters were determined by a linear least-squares fit of the data using weights proportional to the initial velocities (Storer & Carey, 1985).

Results and Discussion

Resonance Raman Spectra and Conformational Properties of the Dithio Ester Model Compounds. The RR spectra of the dithio esters based on Phe-Gly, Gly-Phe-Gly, and Gly-Gly-Phe-Gly in H_2O containing 2–5% CH_3CN are compared in Figure 1 to the RR spectrum of *N*-(β-phenylpropionyl)-glycine ethyl dithio ester. In hydrogen-bonding solvents, *N*-acylglycine dithio esters such as the *N*-(β-phenylpropionyl) analogue assume two major conformational states designated

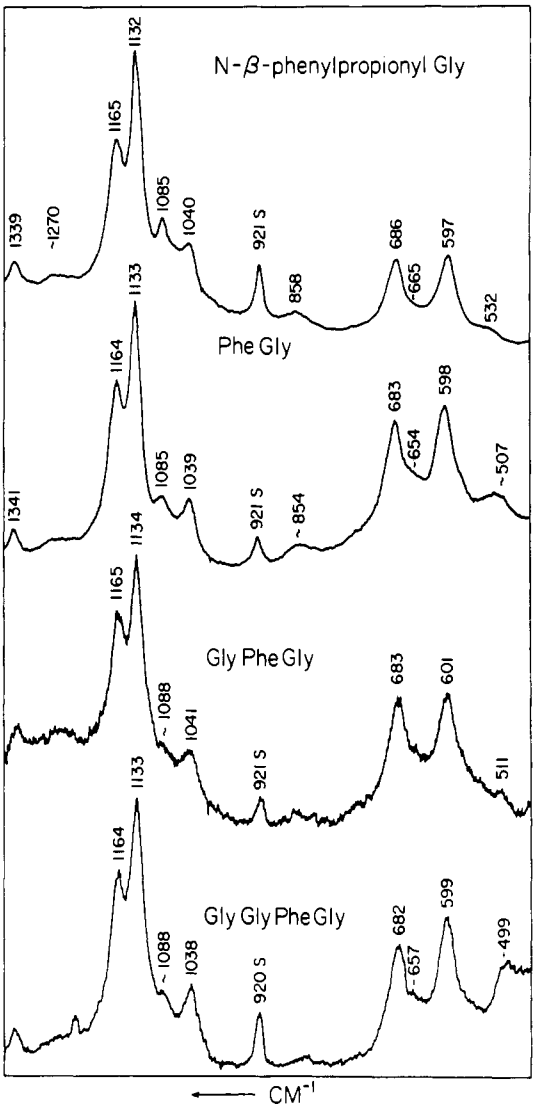

FIGURE 1: Resonance Raman spectra of dithio esters in water (from top to bottom): $C_6H_5(CH_2)_2C(=O)NHCH_2C(=S)SC_2H_5$, $CH_3OC(=O)$-Phe-$NHCH_2C(=S)SC_2H_5$, $CH_3OC(=O)$-Gly-Phe$NHCH_2C(=S)SC_2H_5$, and $CH_3OC(=O)$-Gly-Gly-Phe-$NHCH_2C(=S)C_2H_5$; each dithio ester is $\approx 5 \times 10^{-4}$ M in H_2O containing 2–5% CH_3CN (giving rise to a peak near 920 cm^{-1} and marked "S"). Spectral conditions: laser, 100 mW, 324 nm; 40–60-s total data acquisition time.

A and B, which are shown in Figure 2. Conformer B is characterized by a small (±10–20°) $NHCH_2$–CS (thiol) torsional angle which results from an attractive interaction between the N and thiol S atoms (Varughese et al., 1984). In conformer A, this torsional angle is close to 172°, and there is contact between the N atom and the thiono (=S) sulfur (Huber et al., 1982). The difference in the $NHCH_2$–CS torsional angles of conformers A and B changes the vibrational coupling within the two forms, and as a consequence, conformers A and B have separate and characteristic RR signatures. These have been studied in detail for *N*-acylglycine dithio esters, $RC(=O)NHCH_2C(=S)SC_2H_5$ (Lee et al., 1983; Carey et al., 1985). The close similarity between the *N*-acylglycine and the di-, tri-, and tetrapeptide dithio ester RR spectra in aqueous solution (Figure 1) means that the single amino acid based and multipeptide-based compounds exhibit the same conformational preference in and near the dithio ester linkages [in the R'C(=O)—NH—CH_2—C(=S)—S—C_2H_5 bonds] and that the spectra in Figure 1 can be analyzed on the basis of the earlier work on the *N*-acyl-

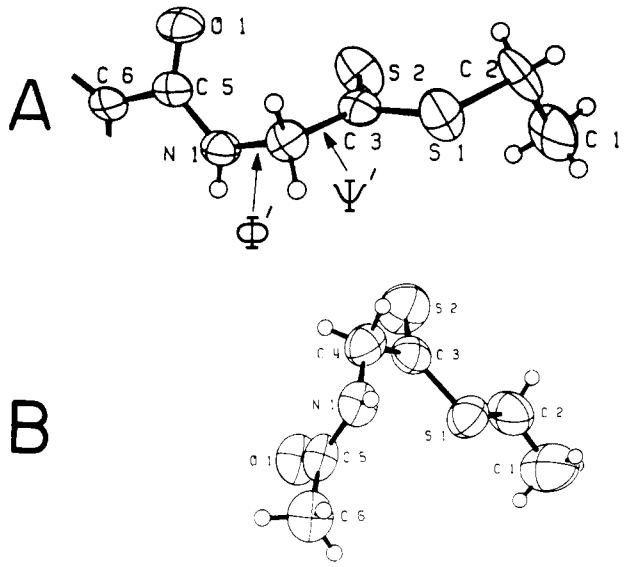

FIGURE 2: Conformer A and conformer B. The torsional angles $NHCH_2$—CS(thiol) (Ψ') and CNH—CH_2C(=S) (Φ') are indicated.

Table I: Summary of the Major Resonance Raman Markers for Conformation

compd	RR features (cm^{-1})	conformer origin
dithio esters in H_2O (Figure 1)	1165	A[a]
	1133	B
	686	A[a]
	660	A
	598	B
dithioacylpapains and cathepsin B's (Figures 4, 6, and 7)	1140	B
	670	B
	590	B

[a] The given conformer makes the major contribution to peak intensity; there may be minor contributions from the other conformer.

glycine derivatives (Lee et al., 1983; Storer et al., 1982).

In Figure 1, the peak near 1165 cm^{-1} is due, in major part, to a conformer A mode that contains substantial contributions from the stretching motions $\nu_{C=S}$ and ν_{C-C} from the CH_2—C(=S) group. The 1133-, 1085-, and 1039-cm^{-1} bands are characteristic conformer B features, and the intense 1133-cm^{-1} peak is an important B conformer marker corresponding to the 1165-cm^{-1} conformer A peak. The peak at 598 cm^{-1} is due to conformer B, while conformer A is responsible for the spectral intensity near 660 cm^{-1} and makes a major contribution to the 683-cm^{-1} profile. This information is summarized in Table I.

X-ray crystallographic data for *N*-acylglycine dithio esters have been crucial in defining their structural properties and for setting up structure–Raman spectra correlations (Huber et al., 1982; Varughese et al., 1984). For the present tri- and tetrapeptide dithio esters, structural data are not available since the compounds have not yet been crystallized as good quality single crystals. However, the RR data for the polycrystalline solids are still informative. The 324-nm excited RR spectrum of the Phe-Gly dithio ester seen in Figure 3 shows evidence for only B modes from a B-type conformer (at 1129, 1043, 607, and 575 cm^{-1}). In contrast, the data for the Gly-Phe-Gly and Gly-Gly-Phe-Gly dithio esters provide evidence for a mixed population of A and B conformers; in addition to the B markers there is increased intensity at 1164 cm^{-1} and in the 670–685-cm^{-1} region, characteristic of a conformer A like population. Furthermore, the ratio of the conformer A to B features changes according to the solvent used to crystallize the material, and this was found for both the Gly-Gly-Phe-Gly and the Gly-Phe-Gly analogues (data are not shown for these experiments). From this it is apparent that as the size of the dithio ester molecules increases, intermolecular forces in the solid become increasingly important in determining the relative populations of the A and B forms.

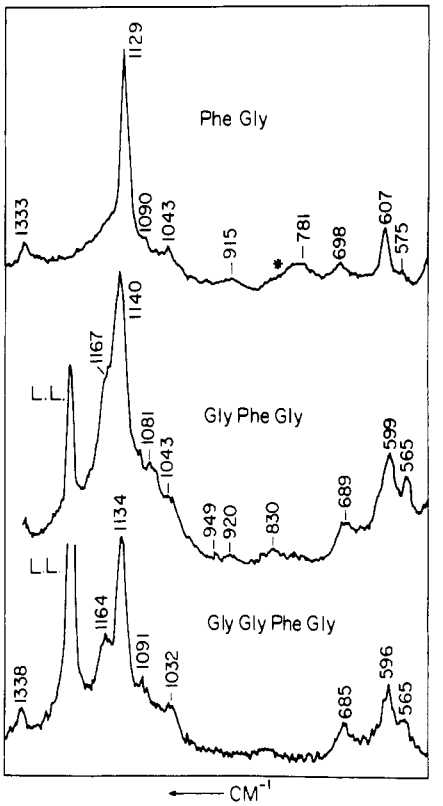

FIGURE 3: Resonance Raman spectra of solid CH_3OC(=O)-Phe-$NHCH_2C$(=S)C_2H_5 (top), CH_3OC(=O)-Gly-Phe-$NHCH_2C$-(=S)SC_2H_5 (middle), and CH_3OC(=O)-Gly-Gly-Phe-$NHCH_2C$-(=S)SC_2H_5 (bottom). Spectral conditions: 45 mW, 324-nm excitation, 60-s total data acquisition time. LL = laser plasma line; quartz, from the sample tube, may make a contribution at the spectral position indicated by an asterisk (*).

Comparison of Raman Spectra of the Dithioacylpapains. The RR spectrum for *N*-(β-phenylpropionyl)glycine dithioacylpapain is compared to the RR spectra of the di-, tri-, and tetapeptide-based dithioacylpapains in Figure 4. With some minor exceptions the spectra for the multipeptide-based dithioacylpapains are very similar, and they bear a resemblance to the spectrum of the *N*-(β-phenylpropionyl)glycine analogue. Each spectrum is dominated by conformer B markers near 1140 and 590 cm^{-1} (the peak at 921 cm^{-1} is due to the CH_3CN used to carry the substrate into solution). Thus, at the first level of approximation, each dithioacyl enzyme is present predominantly as a B population.

The differences among the RR spectra of the Phe-Gly-, Gly-Phe-Gly-, and Gly-Gly-Phe-Gly-papain intermediates are slight and involve minor features; for example, there are differences in the 1065-cm^{-1} spectral region, and the shoulder near 568 cm^{-1} becomes more pronounced through the series Phe-Gly, Gly-Phe-Gly, and Gly-Gly-Phe-Gly (Figure 4). However, the differences between these spectra, taken as a class, and the RR spectrum of the *N*-(β-phenylpropionyl)-glycine analogue are more substantive and involve small but significant changes in the major spectral bands. The main conformer B marker occurs at 1141–1142 cm^{-1} in the Phe-Gly-, Gly-Phe-Gly-, and Gly-Gly-Phe-Gly-based intermediates but at 1138 cm^{-1} in the *N*-(β-phenylpropionyl)glycine deriv-

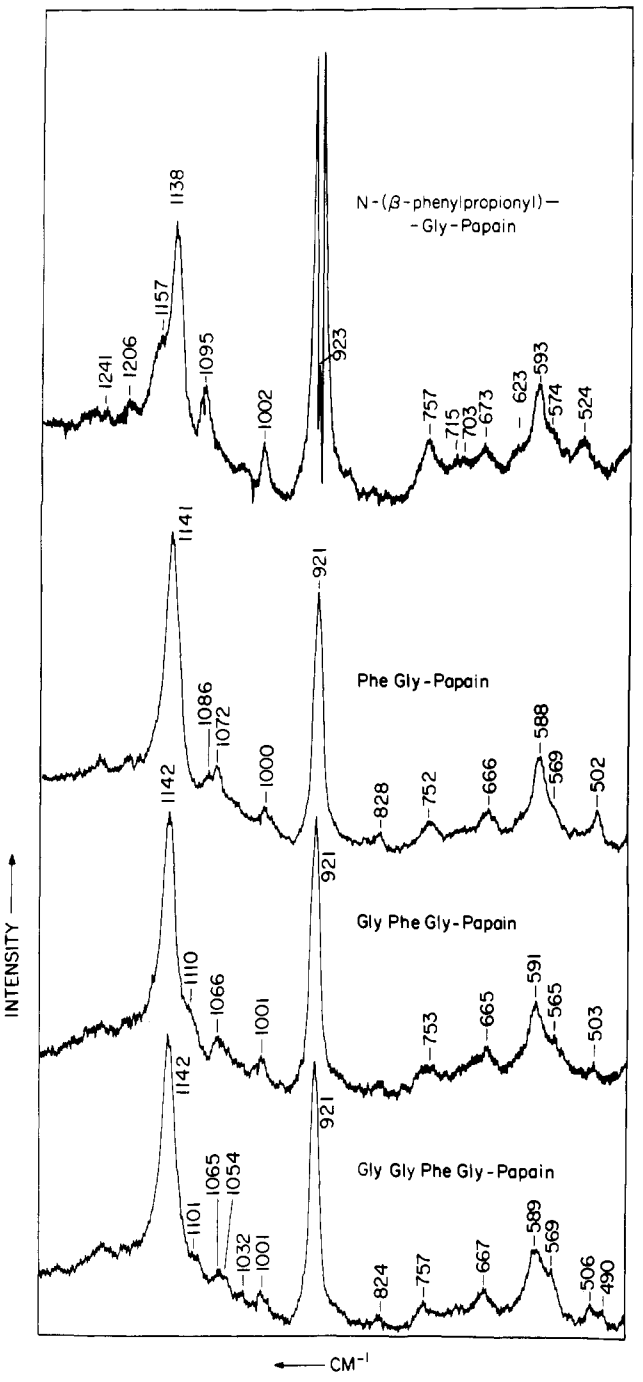

FIGURE 4: Resonance Raman spectra of dithioacylpapains (from top to bottom): $C_6H_5(CH_2)_2C(=O)NHCH_2C(=S)S$-papain, $CH_3OC(=O)$-Phe-$NHCH_2C(=S)$-papain, $CH_3OC(=O)$-Gly-Phe-$NHCH_2C(=S)S$-papain, and $CH_3OC(=O)$-Gly-Gly-Phe-$NHCH_2C(=S)S$-papain. Note the small shift in the peaks near 1140 and 670 cm^{-1} upon going from the top spectrum to the di-, tri-, or tetrapeptide substrates. Concentrations: 140 μM papain, pH 6.0, 1 mm EDTA, and 5 mM substrate, (added in 50% H_2O/CH_3CN; final CH_3CN = 10%). Spectral conditions: laser, 120 mW, 324 nm; 20-s total data acquisition time. CH_3CN features occur at 920, 750 (weak), and 1035 (very weak) cm^{-1}.

ative (Figure 4). The conformer B marker at 588–591 cm^{-1} for the peptides' acyl enzyme spectra occurs at 593 cm^{-1} in the *N*-(β-phenylpropionyl)glycine derivative. Also, the latter intermediate has a shoulder at 1157 cm^{-1} and a medium intensity peak seen at 1095 cm^{-1} that are absent or very weak in the RR spectra of the other acyl enzymes. A further significant difference involves the 673-cm^{-1} peak for the *N*-(β-phenylpropionyl)glycine shifting to 665–667 cm^{-1} for the other dithioacyl enzymes.

The shift of the 1138-cm^{-1} peak in the *N*-(β-phenylpropionyl)glycine papain spectrum to 1141–1142 cm^{-1} in the RR spectra of the multipeptide analogues is associated with changes in the $NH—CH_2—C(=S)$ torsional angles and is discussed in the following section. The shoulder at 1157 cm^{-1} and the peak at 1095 cm^{-1} in the spectrum of the *N*-(β-phenylpropionyl)glycine dithioacyl enzyme (Figure 4) are complex features due to modes delocalized in the $—C(=O)NHCH_2C(=S)S$ fragment (Storer et al., 1983). Spectral changes seen in D_2O demonstrate that these bands contain contributions from the —C(=O)NH— moiety. When the *N*-(β-phenylpropionyl)glycine group is extended to Phe-Gly, to Gly-Phe-Gly, and to Gly-Gly-Phe-Gly, the $—C(=O)NHCH_2C(=S)$ amide group will vibrationally couple to its peptide neighbor, resulting in a change in the normal-mode structure of the 1158- and 1095-cm^{-1} features. Thus, the changes in the 1158- and 1095-cm^{-1} bands seen in Figure 4 could represent a change in bonding about the $—C(=O)NHCH_2C(=S)$ peptide linkages or a redistribution of the normal mode structure due to the addition of further peptide groups.

The third difference between the *N*-(β-phenylpropionyl)glycine intermediate spectrum and the spectra based on the di-, tri-, and tetrapeptide-based substrates in Figure 4 concerns the peak near 670 cm^{-1}. This peak has a high degree of ν_{C-S} character from the cysteine-25 C–S bond (Storer et al., 1983). The ≈7-cm^{-1} shift seen in Figure 4 demonstrates that a change in the $C(=S)S—CH_2C$ torsional angle occurs when additional peptide residues are added to the *N*-(β-phenylpropionyl)glycine moiety. Normal-coordinate analysis indicates that this angle is the major determinant of the ν_{C-S} peak position (Jardim-Barreto et al., 1985). Combined X-ray crystallographic and Raman analyses of *N*-benzoylglycine ethyl dithio ester and *N*-(*p*-chlorobenzyl)glycine ethyl dithio ester (Varughese et al., 1984) indicate that ν_{C-S} shifts from 700 to 680 cm^{-1} when the $C(=S)S—CH_2C$ torsional angle changes from ≈180° to ≈90°. Although this result cannot be extrapolated to quantify the ≈7-cm^{-1} change seen in Figure 4, the qualitative result is clear, namely, that extension of the substrate to a dipeptide and beyond leads to a change in the cysteine $C(=S)S—CH_2C$ torsional angle. Thus, enzyme–substrate contacts far from the S–C bond bring about a change in conformation of this critical linkage.

The high-quality RR data seen in Figure 4 provide the opportunity of comparing the line shapes of the 1141-cm^{-1} band of the Phe-Gly, Gly-Phe-Gly and Gly-Gly-Phe-Gly intermediates. Since broadened RR line shapes can reflect conformational heterogeneity (Carey et al., 1973), the line shape measurement was undertaken to investigate the possibility that extending the acyl chain length might cause a different range of population states to exist in the active site. The position of the 1141-cm^{-1} feature is dependent on the torsional angles in the $RC(=O)NH—CH_2—C(=S)$ fragment (Huber et al., 1982), and these angles change [possibly in a correlated fashion; see the following section and Varughese et al. (1984)] upon going from the acyl enzyme to the tetrahedral intermediate for deacylation. As in any protein molecule, dynamical excursions about the torsional angles (Karplus & McCammon, 1981) occur for the acyl enzyme population, and if these excursions vary markedly along the Phe-Gly, Gly-Phe-Gly, and Gly-Gly-Phe-Gly dithioacyl enzyme series, this could cause differential broadening of the 1141-cm^{-1} line. Careful measurement of the line shape of the three acyl enzymes revealed no differences. Unfortunately, as is argued elsewhere, the major spectroscopic and kinetic discontinuities

Table II: Kinetic Parameters for the Hydrolysis of Methyl Ester Substrates by Papain and Methyl Thiono Ester Substrates by Papain and Cathepsin B[a]

substrate	papain		cathepsin B	
	k_{cat} (s^{-1})	k_{cat}/K_m (M^{-1} s^{-1})	k_{cat} (s^{-1})	k_{cat}/K_m (M^{-1} s^{-1})
N-(β-phenylpropionyl)glycine[b]				
methyl ester	4.73 ± 0.20	714 ± 25		
methyl thiono ester	0.165 ± 0.008	2590 ± 31		
$CH_3OC(=O)$-Phe-Gly				
methyl ester	6.2 ± 0.7	35800 ± 3500 (3)		
methyl thiono ester	0.53 ± 0.03	44100 ± 9800 (3)	1.15 ± 0.15	6670 ± 1400 (3)
$CH_3OC(=)$-Gly-Phe-Gly				
methyl ester	11.3 ± 1.9	59000 ± 10000 (6)		
methyl thiono ester	0.51 ± 0.03	56000 ± 13000 (2)	1.28 ± 0.08	10726 ± 1810 (2)
$CH_3OC(=O)$-Gly-Gly-Phe-Gly				
methyl ester	10.4 ± 0.7	44000 ± 7000 (3)		
methyl thiono ester	0.67 ± 0.06	68200 ± 8450 (2)	1.19 ± 0.02	8020 ± 1050 (2)

[a] All studies were done at 20 °C, an ionic strength of 0.3, and a pH of 6.0. The errors expressed are the higher of the two values obtained by calculating the standard deviation (SD) of the individual values of the kinetic constants or from combinations of the SD's for the individual data sets. In this way both the random experimental error in the data sets and the systematic error between data sets (number of data sets in parentheses) are taken into account. [b] Values taken from Storer and Carey (1985).

are seen between the *N*-(β-phenylpropionyl)glycine and the di-, tri-, and tetrapeptide-based substrates, but the appearance of the 1157-cm^{-1} shoulder for the *N*-(β-phenylpropionyl)-glycine intermediate precludes measurement of the line shape for the 1138-cm^{-1} feature due to this species.

Correlation of Raman Spectral Properties and k_{cat} Values for the Dithioacylpapains. The k_{cat} and k_{cat}/K_m values for the papain-catalyzed hydrolysis of the methyl ester and thiono ester derivatives of *N*-(β-phenylpropionyl)glycine and the Phe-Gly-, Gly-Phe-Gly-, and Gly-Gly-Phe-Gly-based substrates are compared in Table II. The *N*-(β-phenylpropionyl)glycine results have been discussed in detail elsewhere (Storer & Carey, 1985); from, for example, the effect of pH on rate constants and proton inventory studies it was concluded that esters and thiono esters are hydrolyzed by essentially the same reaction pathway. It is apparent from Table II that the differences in the kinetic parameters for ester and thiono ester substrates become less pronounced as the size of the substrate is increased. It is likely that the unfavorable C=S–active site contacts become a smaller percentage of the overall energetics of catalysis as the substrate size increases.

Considering the thiono ester data in Table II, while the k_{cat} and k_{cat}/K_m values for the Phe-Gly, Gly-Phe-Gly, and Gly-Gly-Phe-Gly substrates are very similar, there is a marked difference between these values and those for the *N*-(β-phenylpropionyl)glycine analogue. The k_{cat}'s increase 3–4-fold and the k_{cat}/K_m's 17–26-fold upon going to the larger substrates. At the present time, it is difficult to discuss the change in k_{cat}/K_m since this is a composite constant and, as such, any change can be due to changes in either binding affinity or rate of acylation or both. However, the smaller increase in k_{cat} is particularly interesting in the present analysis because we can equate k_{cat} with k_3, the rate constant for deacylation (Storer & Carey, 1985). Thus, there are changes in both the rate of deacylation and the RR spectra of the dithioacylpapains in going from the *N*-(β-phenylpropionyl)glycine derivative to the intermediates based on the di-, tri-, and tetrapeptides.

Two differences between the RR spectrum (Figure 4) of the *N*-(β-phenylpropionyl)glycine dithioacylpapain and the spectra of the di-, tri-, and tetrapeptide dithioacylpapains concern the shifts in the peaks near 1140 and 665 cm^{-1}. The latter shift is ascribed to a difference in the $C(=S)S—CH_2C$ torsional angle in the dithioacyl enzyme, while for the 1140-cm^{-1} feature there are several lines of evidence, such as joint X-ray crystallographic and Raman studies (Huber et al., 1982; Varughese et al., 1984) and normal-coordinate analysis on model compounds (Jardim-Barreto et al., 1985), which suggest that a major factor affecting the position of the 1140-cm^{-1} peak is the magnitude of the $NHCH_2—CS$(thiol) torsional angle, designated Ψ′. For example, for all known B-conformers (Huber et al., 1982; Varughese et al., 1984; and *N*-(β-phenylpropionyl)glycine ethyl dithio ester, unpublished work from this laboratory) this torsional angle lies between ±20°, and the intense RR peak occurs in the 1120–1145-cm^{-1} region. However, upon going to an A-conformer where the Ψ′ was found to be −172°, the intense RR feature shifts to 1169 cm^{-1} (Huber et al., 1982). Similarly, small shifts in Ψ′ for the closely related *N*-benzoylglycine and *N*-(*p*-chlorobenzoyl)-glycine ethyl dithio esters, from −12° to 9°, results in a small shift of the intense RR feature from 1120 to 1124 cm^{-1}, respectively (Varughese et al., 1984). Moreover, RR data for ethyl dithioacetate (Ozaki et al., 1982) indicate that the intense feature in the 1150-cm^{-1} region is not sensitive to changes in the $CH_3C(=S)S—CH_2CH_3$ torsional angle. Taking these considerations together, the favored explanation for the small variation in the 1140-cm^{-1} peak seen in Figure 4 is a small difference in the $NHCH_2—C(=S)$ torsional angle.

For a series of crystalline *N*-acylglycine dithio esters it has been demonstrated recently that there is a correlation between the $NHCH_2—CS$(thiol) (Ψ′) and $CNH—CH_2C(=S)$ (designated Φ′) torsional angles. The Ψ′ and Φ′ angles are indicated in Figure 2. The Ψ′, Φ′ correlation is shown in Figure 5, where one point has been added to the original four published data points (Varughese et al., 1984). The Ψ′, Φ′ points lie close to a straight line, demonstrating that a variation in, e.g., Ψ′ is compensated by a change in Φ′ in order to preserve a preferred line of approach of the glycine N and thiol S atoms. It was also suggested that Ψ′ and Φ′ might change in a correlated fashion as the acyl enzyme starts to move along the reaction pathway toward the tetrahedral intermediate for deacylation (Varughese et al., 1984). The Ψ′, Φ′ region for the latter is indicated in Figure 5 and is derived from X-ray crystallographic studies of papain (Drenth et al., 1976) and from computer graphics modeling studies (unpublished work, this laboratory).

Since we have interpreted the differences in the 1140-cm^{-1} peak positions seen in Figure 4 in terms of a change in Ψ′, the question now arises as to whether the change in Ψ′ for the di-, tri-, and tetrapeptide-based acyl enzymes means that these intermediates lie in a Ψ′, Φ′ region closer to the tetrahedral intermediate for deacylation than the *N*-(β-phenylpropionyl)glycine dithioacyl enzyme. To explore this question, it is necessary to utilize a correlation between changes in the 1140-cm^{-1} peak position and in Ψ′ and Φ′ (where Ψ′ is

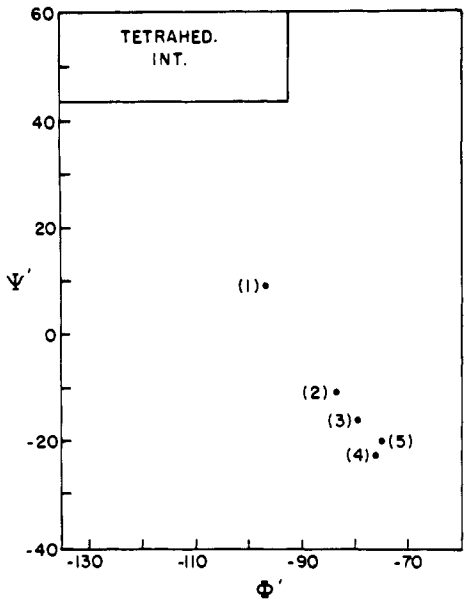

FIGURE 5: A Ψ', Φ' plot. Ψ' is the $NHCH_2$—CS(thiol) torsional angle, and Φ' is the C(=O)NH—CH_2C torsional angle. The Ψ', Φ' values are indicated for *N*-(*p*-chlorobenzoyl)glycine ethyl dithio ester (1), *N*-benzoylglycine ethyl dithio ester (2 and 3), *N*-acetylglycine ethyl dithio ester (4), and *N*-(β-phenylpropionyl)glycine ethyl dithio ester (5). Structure 5 is from unpublished work, this laboratory. The calculated region for the Ψ', Φ' values for the tetrahedral intermediate for deacylation is also indicated.

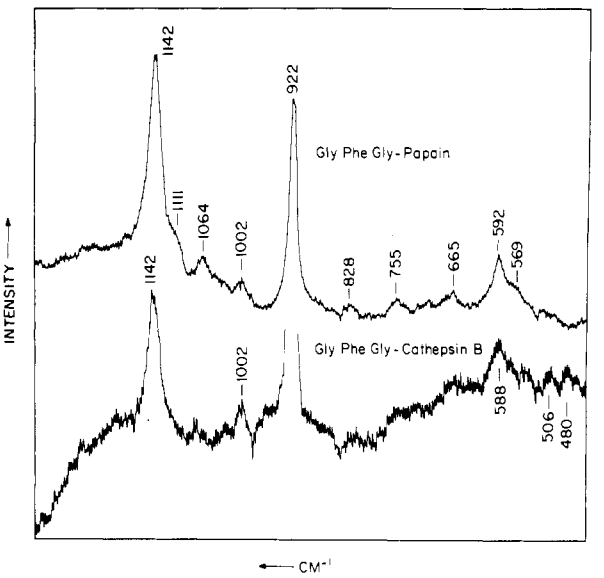

FIGURE 6: Comparison of the RR spectra of $CH_3OC(=O)$-Gly-Phe-$NHCH_2C(=S)S$-papain and -cathepsin B: the spectra are identical within the limits of experimental error. Spectral conditions: 120 mW, 324-nm excitation, 20-s data acquisition time. Active enzyme concentrations were approximately 2 mg/mL in both cases.

probably the dominant factor). At present there is insufficient data to establish such a correlation. However, the present work certainly suggests that a small increase in frequency of the 1140-cm^{-1} feature, taken with the small decrease in frequency of the feature near 670 cm^{-1}, corresponds to a more reactive dithioacyl enzyme since these peak position changes correspond to an increase in k_3 of approximately 3-fold.

The foregoing discuss the concept of increased rectivity and RR spectral changes in a series of dithioacyl enzymes. It is also worth noting that small differences in the position of the RR peak near 1140 cm^{-1} occur consistently for all dithioacylpapains and their corresponding ethyl dithio esters studied thus far. For each of the 20 *N*-acylglycine dithiopapains examined to date, the position of the main peak in the 1130–1140-cm^{-1} region is always a few wavennumbers *higher* than that found for the corresponding model compound in solution or the solid phase [Carey and Storer (1984, 1985) and references cited therein]. Thus, the change in the 1140-cm^{-1} position in going from the model compounds to dithioacyl enzymes is in the same direction as that seen for the increasingly reactive di-, tri-, and tetrapeptide-based dithioacyl enzymes over the *N*-(β-phenylpropionyl)glycine acyl enzyme (Figure 4). Although it is difficult to eliminate all sources of alternative explanations for observed small frequency shifts in vibrational peak positions, in the present instance we can eliminate two alternative reasons for the increase in $\nu_{C=S}$ in the dithioacylpapains over the values seen in the model compounds. First, the increase is unlikely to be due to H bonding or dipolar effects since for model dithio esters' $\nu_{C=S}$ drops to *lower* frequency by a few cm^{-1} in going from CCl_4 to H_2O (Storer et al., 1982). Second, the observed increase in $\nu_{C=S}$ cannot be ascribed to a change in the C(=S)S—CH_2 torsional angle since it is known that $\nu_{C=S}$ is insensitive to this parameter (Ozaki et al., 1982). Thus, the preferred interpretation is that small, energetically inexpensive differences occur between the Ψ' and Φ' angles for *N*-acylglycine ethyl dithio esters and the corresponding dithioacylpapains. We cannot presently state whether these changes are in the direction toward or away from the Ψ', Φ' values for the tetrahedral intermediate (Figure 5).

The present data point to the importance of the amide group linking the P_2 and P_3 sites in the substrate. The common structural difference between the Phe-Gly, the Gly-Phe-Gly, or the Gly-Gly-Phe-Gly intermediate and the *N*-(β-phenylpropionyl)glycine dithioacyl enzyme is the presence of the additional —C(=O)NH— group at the P_2–P_3 link in the former series. Thus, the "discontinuity" in RR and kinetic properties is ascribed to enzyme–substrate contacts at this point, which bring about additional conformational activation near the scissile linkage in the acyl enzyme.

Resonance Raman and Kinetic Data for Dithioacyl Intermediates Involving Cathepsin B. A comparison of the RR and kinetic properties of $CH_3OC(=O)$-Phe-Gly-C(=S)S-papain and $CH_3OC(=O)$-Phe-Gly-C(=S)S-cathepsin B demonstrated marked similarities in the properties of the two dithioacyl enzymes and that the deacylation process common to plant cysteine proteases has been conserved for the mammalian enzyme cathepsin B (Carey et al., 1984). This comparison is extended in the present study to include the $CH_3OC(=O)$-Gly-Phe-Gly- and $CH_3OC(=O)$-Gly-Gly-Phe-Gly-based substrates. Figure 6 compares the RR spectra of the dithioacyl enzyme formed from the $CH_3OC(=O)$-Gly-Phe-Gly substrate and papain and porcine spleen cathepsin B, and Figure 7 compares the corresponding RR spectra with the $CH_3OC(=O)$-Gly-Gly-Phe-Gly substrate. The RR spectra from the intermediates involving cathepsin B are of inferior quality to those from papain intermediates, due in part to the fact that approximately half of the cathepsin B preparation contains inactive material (Barrett & Kirschke, 1981), whereas for papain the catalytically inactive portion makes up 10% or less of the total protein. However, it is clear that, just as in the case of the intermediates involving CH_3OC-(=O)-Phe-Gly (Carey et al., 1984), the RR spectra of the cathepsin B dithioacyl enzymes are identical with those for the intermediates involving papain. Thus, the conclusions enunciated above, and elsewhere (Carey & Storer, 1984, 1985), for the dithioacylpapains apply also to the dithioacyl cathepsin B's. Both enzymes bind the substrates in a B-type conformation about the —$C(=O)NHCH_2C(=S)SCH_2$

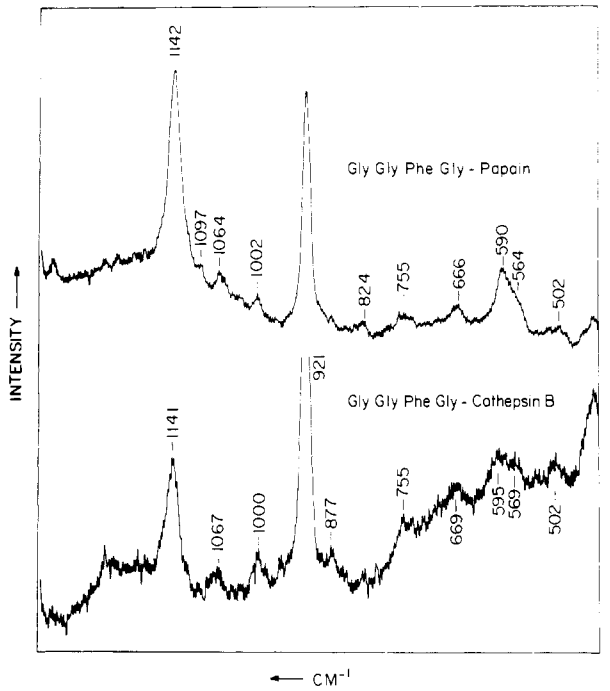

FIGURE 7: Comparison of the RR spectra of $CH_3OC(=O)$-Gly-Gly-Phe-$NHC(=O)CH_2C(=S)S$-papain and -cathepsin B: the spectra are identical within the limits of experimental error. Spectral conditions: 120 mW, 324-nm excitation, 20-s data acquisition time. Active enzyme concentrations were approximately 2 mg/mL in both cases.

linkages. The $NHCH_2$–CS (thiol) torsional angles lie between $\pm(20 \pm 10°)$, the dithio ester groups are *S*-cis and planar, and the CS–CH_2C torsional angles are probably in the region either 90° or −90°, and in each case the values are the same or very similar for dithioacyl enzyme intermediates involving papain or cathepsin B. There is no evidence for any feature in the RR spectra, in Figure 6 or 7, that is due to a conformer other than conformer B. There is the possibility, especially in the poorer quality cathepsin B intermediate spectra, that a small percentage of the total population exists in a non-B form and is undetected; if this population had a conformer A like spectral signature, we estimate that this percentage cannot exceed 10% in the case of the cathepsin B or 5% in the case of the papain dithioacyl enzymes.

At the signal-to-noise ratio achieved in Figures 6 and 7 we consider each dithioacylcathepsin B spectrum to be identical with that for the corresponding papain intermediate. Since the positions of the bands near 1140, 670, and 595 cm^{-1} are known to be sensitive to changes in torsional angles in the $NH—CH_2—C(=S)—S—CH_2$ fragment, these angles must be the same or very similar for each substrate in papain's and cathepsin B's active site. These strong structural similarities in the catalytically crucial bonds are echoed by similarities in the rate constants for deacylation for the papain and cathepsin B acyl enzymes. Table II lists the k_{cat} and k_{cat}/K_m values for the multipeptide thiono ester hydrolysis catalyzed by papain and cathepsin B. For thiono esters of the type listed in Table II $k_{cat} = k_3$, the rate constant for deacylation. Thus, from Table II the rate constants for deacylation from cathepsin B are very similar and are 2–4-fold higher than those for the corresponding papain dithioacyl enzymes. Since we have argued that each substrate takes up an essentially identical conformation in the $—NHCH_2C(=S)SCH_2—$ fragment in papain's and cathepsin B's active site, we ascribe the higher k_{cat} for the cathepsin B case to slight differences in orientation or reactivity of the catalytically active side chains in the active sites (Willenbrock & Brocklehurst, 1984).

ACKNOWLEDGMENTS

It is a pleasure to acknowledge the technical assistance of P. Berti, R. G. Carriere, and L. R. Sans Cartier.

Registry No. $Ph(CH_2)_2CONHCH_2C(=S)SPh$, 101653-88-7; (*S*)-MeOCO-Phe-$NHCH_2C(=S)SPh$, 101653-89-8; (*S*)-MeOCO-Gly-Phe-$NHCH_2C(=S)SPh$, 101653-90-1; (*S*)-MeOCO-Gly-Gly-Phe-$NHCH_2C(=S)SPh$, 101653-91-2; L-MeOCO-Phe-Gly-OMe, 101653-92-3; L-MeOCO-Gly-Phe-Gly-OMe, 101653-93-4; L-MeO-CO-Gly-Gly-Phe-Gly-OMe, 101653-94-5; papain, 9001-73-4; cathepsin B, 9047-22-7; cysteine proteinase, 37353-41-6.

REFERENCES

Anderson, G. W., Zimmerman, J. E., & Callahan, F. M. (1967) *J. Am. Chem. Soc. 89*, 5012–5017.

Barrett, A. J., & Kirschke, H. (1981) *Methods Enzymol. 80*, 535–561.

Carey, P. R., & Sans Cartier, L. R. (1983) *J. Raman Spectrosc. 14*, 271–275.

Carey, P. R., & Storer, A. C. (1984) *Annu. Rev. Biophys. Bioeng. 13*, 25–49.

Carey, P. R., & Storer, A. C. (1985) *Pure Appl. Chem. 57*, 225–234.

Carey, P. R., Froese, A., & Schneider, H. (1973) *Biochemistry 12*, 2198–2208.

Carey, P. R., Angus, R. H., Lee, H., & Storer, A. C. (1984) *J. Biol. Chem. 259*, 14357–14360.

Carey, P. R., Lee, H., Ozaki, Y., & Storer, A. C. (1985) *J. Mol. Struct. 126*, 261–270.

Drenth, J., Kalk, K. H., & Swen, H. M. (1976) *Biochemistry 15*, 3731–3738.

Huber, C. P., Ozaki, Y., Pliura, D. H., Storer, A. C., & Carey, P. R. (1982) *Biochemistry 21*, 3109–3115.

Jardim-Barreto, V. M., Carey, P. R., Storer, A. C., & Teixeira-Dias, J. J. C. (1984) *Port. J. Chem. 26*, 131–142.

Karplus, M., & McCammon, J. A. (1981) *CRC Crit. Rev. Biochem. 9*, 293–349.

Lee, H., Storer, A. C., & Carey, P. R. (1983) *Biochemistry 22*, 4781–4789.

Lowe, G., & Yuthavong, Y. (1971) *Biochem. J. 124*, 107–115.

Ozaki, Y., Storer, A. C., & Carey, P. R. (1982) *Can. J. Chem. 60*, 190–198.

Schecter, I., & Berger, A. (1968) *Biochem. Biophys. Res. Commun. 32*, 898–902.

Storer, A. C., & Carey, P. R. (1985) *Biochemistry 24*, 6808–6818.

Storer, A. C. Ozaki, Y., & Carey, P. R. (1982) *Can. J. Chem. 60*, 199–209.

Storer, A. C., Lee, H., & Carey, P. R. (1983) *Biochemistry 22*, 4789–4796.

Thompson, R. C. (1974) *Biochemistry 13*, 5495–5501.

Varughese, K. I., Storer, A. C., & Carey, P. R. (1984) *J. Am. Chem. Soc. 106*, 8252–8257.

Venkatasubban, K. S., & Schowen, R. L. (1984) *CRC Crit. Rev. Biochem. 17*, 1–44.

Willenbrock, F., & Brocklehurst, K. (1984) *Biochem. J. 222*, 805–814.